JOURNAL OF MATERIALS SCIENCE 28 (1993) 4299–4304

Analysis of high-loss viscoelastic composites

C. P. CHEN, R. S. LAKES*‡
*Department of Mechanical Engineering, and *Department of Biomedical Engineering and *Center for Laser Science and Engineering, University of Iowa, Iowa City, IA 52242, USA*

A theoretical study of the viscoelastic properties of composites is presented with the aim of identifying structures which give rise to a combination of high stiffness and high loss tangent. Laminates with Voigt and Reuss structures, as well as composite materials attaining the Hashin–Shtrickman bounds on stiffness were evaluated by the correspondence principle. Similarly, viscoelastic properties of composites containing spherical or platelet inclusions were explored. Reuss laminates and platelet-filled materials composed of a stiff, low-loss phase and a compliant high-loss phase were found to exhibit high stiffness combined with a high loss tangent.

1. Introduction

Viscoelastic materials can be of use in the damping of mechanical vibration and in the absorption of sound. The loss tangent, or tangent of the phase angle, δ, between stress and strain in sinusoidal loading, is a useful measure of material damping. Most materials used in structural applications, however, have small loss tangents. Conversely, materials with high loss tangents tend to be compliant, and hence they are not of structural interest. Fig. 1 contains a stiffness–loss map (plot of the absolute value of the dynamic modulus versus the loss tangent) for some representative materials. Compliant, lossy materials are used as layers over stiff materials in various applications; nevertheless, a stiff material with high loss would be of use in the structural damping of noise and vibration. This article considers the possibility of making composite microstructures providing high stiffness and high loss.

A possible avenue for making high-loss composites is to make use of non-affine deformation. This is in contrast to affine deformation in which the particles in the solid move in a way corresponding to a uniform strain plus a rotation in a continuum. The materials developed by Lakes [1] with negative Poisson's ratios exhibit this property in that foam cells unfold during deformation [2, 3]. Non-affine deformation can result in high viscoelastic loss in a composite if the phase which has the highest loss experiences a larger strain than does the composite as a whole.

The elastic properties of multi-phase composite materials have been studied extensively. Of these studies, the most relevant to the present work are those dealing with bounds on the elastic behaviour and predicted properties of composites of relatively simple structure. The upper and lower bounds of stiffness of two-phase and many-phase composite materials have been obtained in terms of the volume fractions of constituents [4, 5]. Bounds and expressions for the effective elastic moduli of materials reinforced by parallel, hollow, circular fibres in hexagonal or random arrays have also been derived by a variational method [4]. Furthermore, bounds on three independent effective elastic moduli of a n-phase fibre-reinforced composite of arbitrary transverse phase geometry (plane-strain bulk modulus, transverse-shear modulus and shear-modulus-in-plane-parallel-to-fibres) have been derived in terms of phase volume fractions [6]. For viscoelastic heterogeneous media of several discrete linear viscoelastic phases with known stress–strain relations, it has been shown that the effective relaxation and creep functions could be obtained by the correspondence principle of the theory of linear viscoelasticity [7]. In some cases explicit results in terms of general, linear, viscoelastic matrix properties have been given, thus permitting the direct use of experimental information [8]. In a review of particulate-reinforcement theories for polymer composites, it was concluded that the macroscopic behaviour was affected by the size, shape, distribution, and interfacial adhesion of inclusions [9]. This article makes use of some of these results for elastic composites in exploring accessible regions of the stiffness–loss maps of the materials.

2. Elastic and viscoelastic properties of composites

For the simplest case of a two-phase composite, the Voigt and Reuss composites described below represent rigorous upper and lower bounds on the Young's modulus for a given volume fraction of one phase. The Hashin–Shtrickman composites represent upper and lower bounds for isotropic elastic composites. Viscoelastic composites containing spherical or platelet inclusions are also considered. Results obtained via the

‡ Author to whom correspondence should be addressed.

0022–2461

correspondence principle are plotted as stiffness–loss maps in Section 3.

2.1. Voigt composite

Let phase 1 denote stiff, and phase 2 denote high loss. The geometry of a Voigt model structure is shown in Fig. 2. The composite can contain laminations as shown in Fig. 2a or it can be made of continuous fibres as in Fig. 2b; in either case the strain in each phase is the same. For an elastic material with one of these structures, the Voigt relation is $E_c = E_1 V_1 + E_2 V_2$, in which E_c, E_1 and E_2 refer to the Young's modulus of the composite, phase 1 and phase 2; and V_1 and V_2 refer to the volume fraction of phase 1 and phase 2, with $V_1 + V_2 = 1$. The Voigt relation for the stiffness of an elastic composite is obtained by recognizing that for the given geometry, the strain in each phase is the same; the forces in each phase are additive.

By the correspondence principle [10, 11], the elastic relation can be converted to a steady state, harmonic, viscoelastic relation by replacing Young's moduli, E, by $E^*(i\omega)$ or E^*, in which ω is the angular frequency of the harmonic loading. This procedure gives

$$E_c^* = E_1^* V_1 + E_2^* V_2 \quad (1)$$

with $E^* = E' + iE''$ and loss tangent $\tan\delta = E''/E'$. Taking the ratio of real and imaginary parts, the loss tangent of the composite, $\tan\delta_c = E_c''/E_c'$, is obtained.

$$\tan\delta_c = \frac{V_1 \tan\delta_1 + V_2(E_2'/E_1')\tan\delta_2}{V_1 + (E_2'/E_1')V_2} \quad (2)$$

2.2. Reuss composite

The geometry of the Reuss-model structure is shown in Fig. 2c; each phase experiences the same stress. For elastic materials, $1/E_c = V_1/E_1 + V_2/E_2$. Again, using the correspondence principle, the viscoelastic relation is obtained as

$$\frac{1}{E_c^*} = \frac{V_1}{E_1^*} + \frac{V_2}{E_2^*} \quad (3)$$

Separating the real and imaginary parts of E_c^*, the loss tangent of the composite, $\tan\delta_c$ is obtained

$$\tan\delta_c = \frac{(\tan\delta_1 + \tan\delta_2)(V_1 + V_2 E_1'/E_2') - (1 - \tan\delta_1\tan\delta_2)(V_1\tan\delta_2 + V_2\tan\delta_1 E_1'/E_2')}{(1 - \tan\delta_1\tan\delta_2)(V_1 + V_2 E_1'/E_2') + (\tan\delta_1 + \tan\delta_2)(V_1\tan\delta_2 + V_2\tan\delta_1 E_1'/E_2')} \quad (4)$$

2.3. Hashin–Shtrickman composite: arbitrary two-phase geometry

Allowing for arbitrary phase geometry, the upper and lower bounds on the elastic moduli as a function of composition have been developed using variational principles. The lower bound for the shear modulus, G_L, of the composite was given in [5] as

$$G_L = G_2 + \frac{V_1}{\dfrac{1}{G_1 - G_2} + \dfrac{6(K_2 + 2G_2)V_2}{5(3K_2 + 4G_2)G_2}} \quad (5)$$

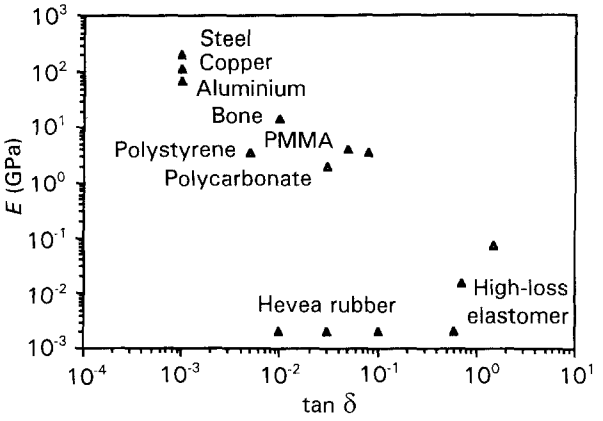

Figure 1 Stiffness versus loss tangent for some representative materials at or near room temperature. Steel, 1 Hz [17]; copper, 600 Hz [17]; polymethyl methacrylate (PMMA), 10 Hz and 1 kHz [18]; bone, 1–100 Hz, [19]; hevea rubber, 10 Hz to 2 kHz [18]; polystyrene, 100 Hz, 1 kHz [18]; polycarbonate, 100 Hz [20]; and viscoelastic elastomer, 100 Hz to 1 kHz [21].

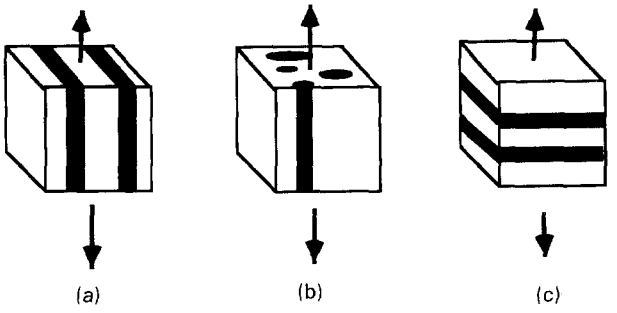

Figure 2 (a) Laminated Voigt structure, (b) fibrous Voigt structure, and (c) Reuss structure.

in which K_1, G_1 and V_1, and K_2, G_2 and V_2 are the bulk modulus, shear modulus and volume fraction of phases 1, and 2, respectively. Here $G_1 > G_2$, so that G_L represents the lower bound on the shear modulus. Interchanging the numbers 1 and 2 in Equation 5 results in the upper bound, G_U, for the shear modulus.

As for viscoelastic materials, if the correspondence principle is applied, then the complex viscoelastic shear moduli of the composite, G_L^* and G_U^*, are obtained as

$$G_L^* = G_2^* + \frac{V_1}{\dfrac{1}{G_1^* - G_2^*} + \dfrac{6(K_2^* + 2G_2^*)V_2}{5(3K_2^* + 4G_2^*)G_2^*}} \quad (6)$$

and

$$G_U^* = G_1^* + \frac{V_2}{\dfrac{1}{G_2^* - G_1^*} + \dfrac{6(K_1^* + 2G_1^*)V_1}{5(3K_1^* + 4G_1^*)G_1^*}} \quad (7)$$

In these cases the loss tangent is more complicated to write explicitly, so it is expedient to graphically display computed numerical values.

2.4. Hashin transversely isotropic fibre-reinforced composite

This case is of interest since it allows more than two phases; a situation applicable to the analysis of experimental results in a companion article. For two phases the results are almost identical to the arbitrary-phase-geometry case considered above. The shear modulus of elastic multi-phase transversely isotropic fibre-reinforced composites of arbitrary transverse phase geometry, can be bounded from below and above in terms of phase moduli and phase volume fractions. The lower and upper bounds on the shear modulus $m^{(-)}$ and $m^{(+)}$ were given for elastic composites in [6] as

$$m^{(-)} = G_1 + \frac{2G_1(K_1 + G_1)}{K_1 + 2G_1} \times \left\{ \left[\sum_{r=2}^{r=n} \frac{(G_r - G_1)V_r}{G_1 + K_1G_1/(K_1 + 2G_1)} \right]^{-1} - 1 \right\}^{-1} \quad (8)$$

and

$$m^{(+)} = G_n + \frac{2G_n(K_n + G_n)}{K_n + 2G_n} \times \left\{ \left[\sum_{r=1}^{r=n-1} \frac{(G_r - G_n)V_r}{G_r + K_nG_n/(K_n + 2G_n)} \right]^{-1} - 1 \right\}^{-1} \quad (9)$$

in which n is the number of the phases, G_1 and K_1 are the shear and bulk moduli of the most compliant phase, G_n and K_n are the shear and bulk moduli of the stiffest phase, r is a free index representing the phase number and phases are numbered in order of increasing stiffness.

On the basis of the correspondence principle, corresponding results for the complex shear modulus (not necessarily bounds) of the composites are again obtained by replacing $m^{(-)}$, $m^{(+)}$, G_1, K_1, G_r and G_n by G_L^*, G_U^*, G_1^*, K_1^*, G_r^* and G_n^* in Equations 8 and 9. The loss tangent is again complicated to write explicitly, so it is graphically displayed using computed numerical values.

2.5. Spherical particulate inclusions

For a small volume fraction $V_2 = 1 - V_1$ of spherical elastic inclusions in a continuous phase of another elastic material, the shear modulus of the composite G_c was given in [12] as

$$\frac{G_c}{G_1} = 1 - \frac{15(1 - \nu_1)(1 - G_2/G_1)V_2}{7 - 5\nu_1 + 2(4 - 5\nu_1)G_2/G_1} \quad (10)$$

in which ν_1 is Poisson's ratio for phase 1; and phase 1 and phase 2 denote the matrix material and the inclusion material, respectively.

Using the correspondence principle again, and assuming there is no relaxation in Poisson's ratio, Equation 10 becomes

$$G_c^* = G_1^* - \frac{15(1 - \nu_1)(G_1^* - G_2^*)V_2}{7 - 5\nu_1 + 2(4 - 5\nu_1)G_2^*/G_1^*} \quad (11)$$

for the complex shear modulus of the composite material. The loss tangent is again complicated to write explicitly, so it is graphically displayed using computed numerical values.

2.6. Platelet inclusions

For a dilute suspension of platelet elastic inclusions of phase 2 in a matrix of phase 1, the shear modulus of the composite G_c was given in [12] as

$$G_c = G_1 + \frac{V_2(G_2 - G_1)}{15} \times \left[\frac{9K_2 + 4(G_1 + 2G_2)}{K_2 + \frac{4}{3}G_2} + 6\frac{G_1}{G_2} \right] \quad (12)$$

Again, using the correspondence principle, Equation 12 becomes

$$G_c^* = G_1^* + \frac{V_2(G_2^* - G_1^*)}{15} \times \left[\frac{9K_2^* + 4(G_1^* + 2G_2^*)}{K_2^* + \frac{4}{3}G_2^*} + 6\frac{G_1^*}{G_2^*} \right] \quad (13)$$

for the complex shear modulus of the composite materials.

As for procedure, although Equations 5–13 were developed for the shear modulus of the composite, the shear moduli, G^*, were replaced by Young's moduli, E^*, in the figures for comparison with Fig. 1. The Voigt and Reuss relations given by Equations 1 and 3 apply to G^* as well as to E^*. The actual relationship between E^* and G^* and the properties of the constituents of a composite is simple only for certain phase geometries. For example, for some common phase geometries, a Poisson's ratio of 0.3 for each phase gives a Poisson's ratio close to or equal to 0.3 for the composite. However for some other phase geometries, a constituent Poisson's ratio of 0.3 can give rise to a negative Poisson's ratio in cellular solids with one phase void [1] or in unusual laminates [13]. The calculations are on the basis that $V_1 + V_2 = 1$ except that $V_1 + V_2 = 0.8$ for the multi-phase Hashin elastic bound, for which a 20% void volume fraction is assumed to be contained as a third phase in the composite.

3. Results and discussion

Results are plotted as stiffness-loss maps (plots of $|E^*|$ versus $\tan\delta$) as shown in Figs 3 to 5.

Fig. 3 shows predicted properties of composites containing phases which differ greatly in properties. Steel is considered as phase 1, with $|E_1^*| = 200$ GPa, $\tan\delta_1 = 0.001$, and a viscoelastic elastomer is phase 2, with $|E_2^*| = 0.020$ GPa, $\tan\delta_2 = 1.0$. The graph of Fig. 3 was enlarged for clarity in the vicinity of 100% phase 1 and is shown in Fig. 4. A small volume fraction of phase 2 results in a large increase in loss with little reduction in stiffness, so that the Reuss structure permits higher losses than the Voigt structure. However, in the Reuss structure each phase carries the full stress, so that a composite of this type will not be strong if, as is usual, the soft phase 2 is weak.

As for bounds on the properties, the curves for the Voigt and Reuss composites enclose a region in the stiffness–loss map, as do the curves for the upper and lower Hashin–Shtrickman composites. It is tempting to think of these curves as bounds on the viscoelastic

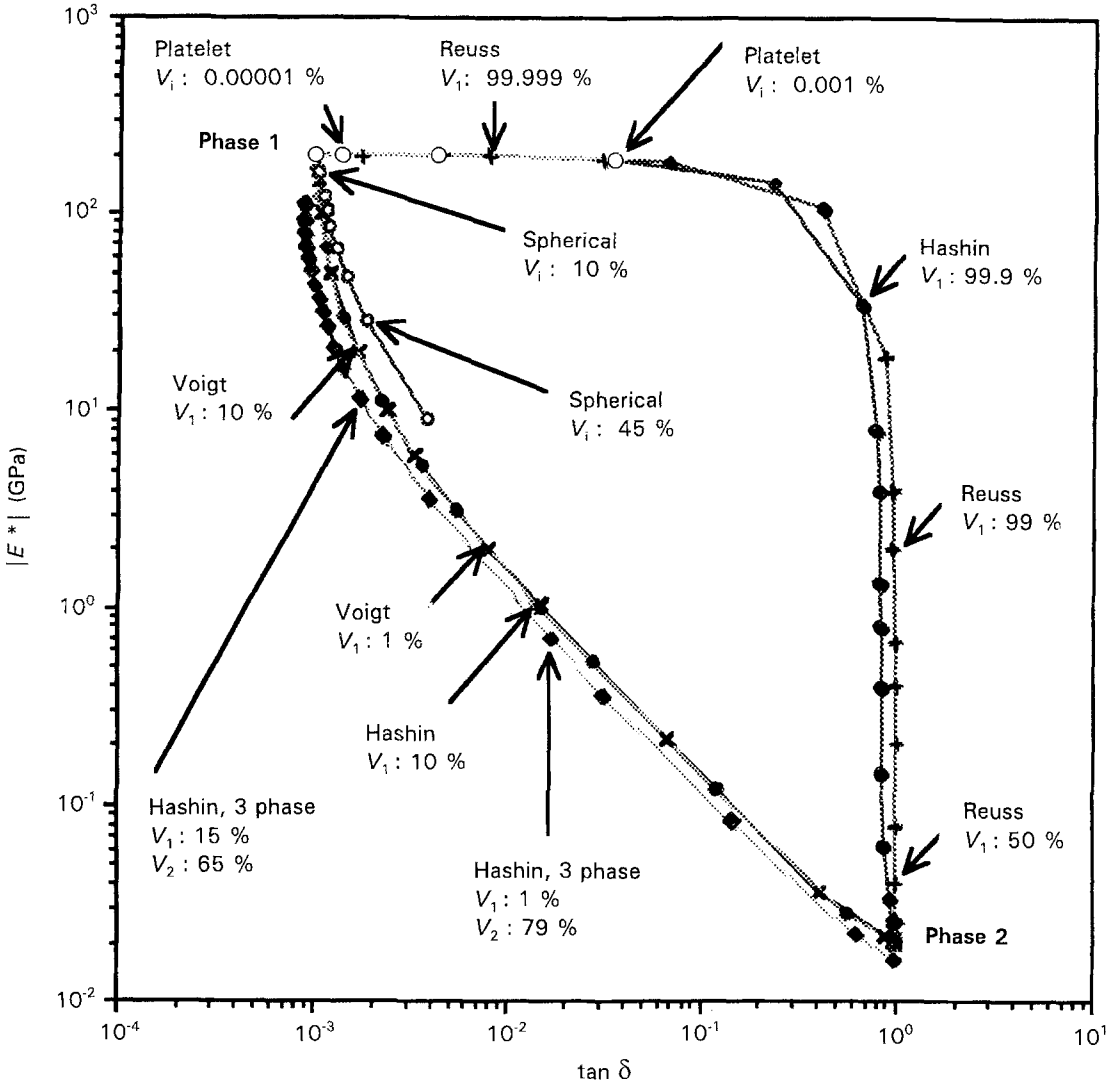

Figure 3 Stiffness–loss map for composites where steel is phase 1 and viscoelastic elastomer is phase 2: (×) Voigt curve, (+) Reuss curve, (◆) two-phase Hashin curve, (◇) upper curve of three-phase Hashin composite with 20% voids as one phase, (○) composite with phase 2 as dilute spherical inclusions, and (□) composite with phase 2 as dilute platelet inclusions. (V_i is the volume of inclusions.)

behaviour; however, such a surmise has not been proven. They represent extremes of composites which can be fabricated; however, it is not yet known if they represent true bounds. The bounds for the real and imaginary parts E' and E'' of the complex modulus of composites has been mathematically established and shown to be equivalent to the Voigt and Reuss relations [14]. Therefore the stiffness, expressed as $|E^*|$ of the composite is bounded from above by the Voigt limit and cannot exceed the stiffness of the stiff phase. This is not quite the same as establishing bounds for a stiffness–loss map since it is not obvious whether a maximum in $\tan\delta = E''/E'$ could be obtained simultaneously with a maximum in E'. In particular, $\tan\delta_c = E''_{\text{Voigt}}/E'_{\text{Reuss}} > E''_{\text{Reuss}}/E'_{\text{Reuss}}$ can be constructed within the bounds of Roscoe. It is not yet known if such a composite is physically realizable.

In the stiffness–loss map, the lower and upper two-phase Hashin composites behave similarly to the Voigt and Reuss composites, respectively. This is in contrast to the usual plots of elastic stiffness against volume fraction, in which the Hashin bounds can differ greatly from the Voigt/Reuss bounds. As for the physical attainment of Voigt and Reuss composites, simple laminates can be made as in Fig. 2, but these are anisotropic. Isotropic composites which attain the Voigt or Reuss moduli are not considered to be attainable. Isotropic polycrystals attaining the Voigt or Reuss bounds for the bulk modulus are also possible [15] at the expense of some added structural complexity.

For the three-phase Hashin structure with a 20% void content in the composite, the lower curve reduces to zero and is not shown in the graph; the upper bound lies close to the Voigt curve with a 20 to 40% lower stiffness as shown in Fig. 3.

The composite containing soft spherical inclusions is also found to behave similarly to the Voigt composite, in that a small volume fraction of soft, viscoelastic material has a minimal effect on the loss tangent, though it does reduce the stiffness. As for the composite containing soft platelet inclusions, it is found that the results are similar to those of the Reuss structure. A small volume fraction of platelet inclusions as phase 2 results in a very large increase in loss tangent without any significant reduction in the stiffness. However, soft platelets resemble penny-shaped cracks in the matrix, so that such a composite would

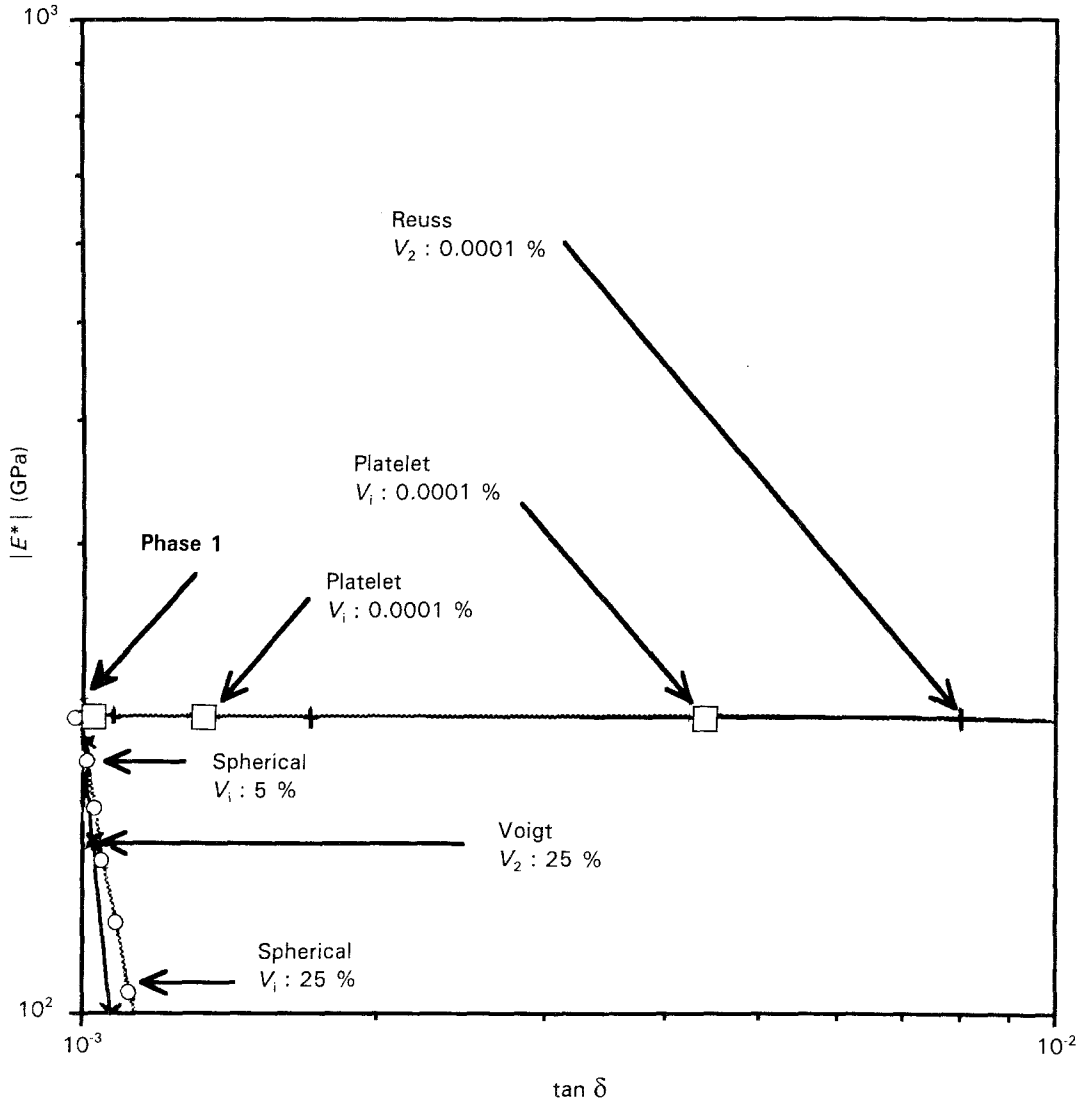

Figure 4 Stiffness–loss map for composites where steel is phase 1 and viscoelastic elastomer is phase 2; this is an expanded plot of the upper left-hand portion of Fig. 3; (×) Voigt curve, (+) Reuss curve, (◇) upper curve of three-phase Hashin composite with 20% voids as one phase, (○) composite with phase 2 as dilute spherical inclusions, and (□) composite with phase 2 as dilute platelet inclusions. (V_i is the volume of inclusions.)

be weaker than the matrix, particularly if the matrix were brittle.

Fig. 5 shows the predicted properties for composites containing phases which differ less in their properties than steel and viscoelastic elastomers. Copper as phase 1, with $|E_1^*| = 117$ GPa, $\tan\delta_1 = 0.002$ and indium as phase 2, with $|E_2^*| = 10.8$ GPa, $\tan\delta_2 = 0.025$ (at 1 kHz) were used for this investigation. Observe that the shape of this stiffness–loss map differs from the case of the polymer–metal composite. The implication of this difference in shape is as follows. If the constituents differ by orders of magnitude in stiffness and loss, then the Reuss and platelet composites are orders of magnitude superior to the Voigt and spherical inclusion composites in achieving high stiffness and high loss. If the constituents do not differ as much in their properties, then their composites of various structures do not differ as much either. Composites containing a stiff, low-loss material (such as a metal) and a small amount of a compliant, high-loss material can exhibit a stiffness close to that of the metal, as well as a high loss superior to that of a metal–metal composite.

An interesting aspect of the Reuss and platelet composites which give the highest loss (for given stiffness) is that they exhibit highly non-uniform strain fields. The strain in the soft, lossy phase is much larger than the strain in the stiff phase. This is in contrast to the Voigt composite in which the strain in each phase is the same. The re-entrant foams [16] with a negative Poisson's ratio also exhibit non-affine deformation of a more complex nature in that the foam cells unfold as the foam is deformed.

4. Conclusions

1. In a stiffness–loss map, the upper and lower two-phase Hashin composites behave similarly to the Voigt and Reuss composites, respectively.

2. Reuss laminates and platelet-filled materials based on a stiff, low-loss phase and a compliant high-loss phase were found to exhibit high stiffness combined with a high loss tangent. However, in the Reuss structure each phase carries the full stress, so that a composite of this type will not be strong if, as is usual, the compliant phase is weak.

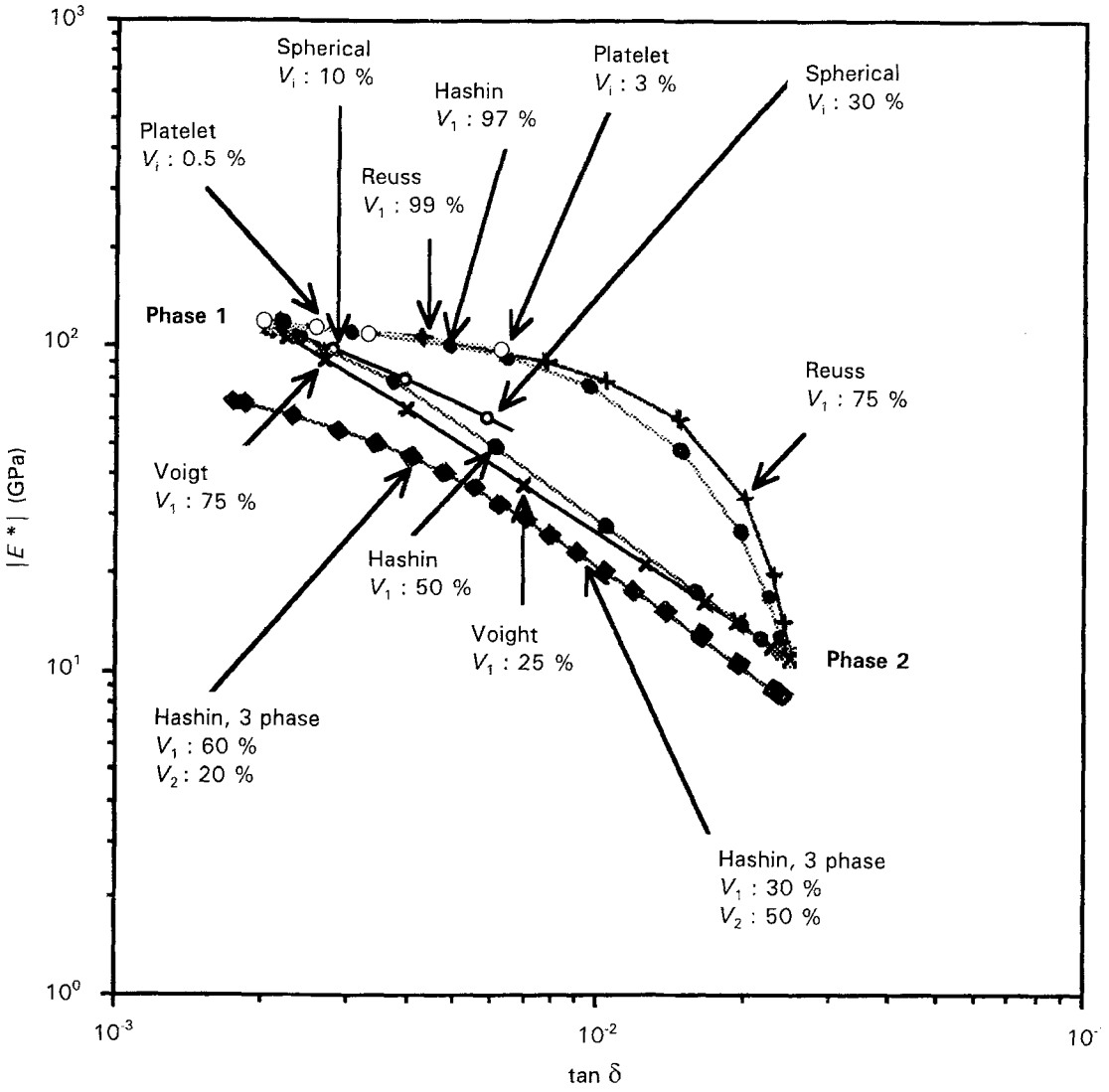

Figure 5 Stiffness–loss map for composites where copper is phase 1 and indium is phase 2: (×) Voigt bound, (+) Reuss curve, (◆) two-phase Hashin curve, (◇) upper curve of three-phase Hashin composite with 20% voids as one phase, (○) composite with phase 2 as dilute spherical inclusions, and (□) composite with phase 2 as dilute platelet inclusions. (V_i is the volume of inclusions.)

3. A composite containing soft lossy spherical inclusions in a stiff matrix behaves similarly to the Voigt composite, i.e. it has low loss and a reduction in stiffness.

4. Composites containing a metal and a small amount of a compliant, high-loss polymer can in principle exhibit a stiffness close to that of the metal, as well as high loss.

Acknowledgements

We thank the ONR for their support of this work. We also thank the University of Iowa for a University Faculty Scholar Award to one of the authors (RSL).

References

1. R. S. LAKES, *Science* **235** (1987) 1038.
2. *Idem, J. Mater. Sci.* **26** (1991) 2287.
3. C. P. CHEN and R. S. LAKES, *J. Mater. Sci.* **26** (1991) 5397.
4. Z. HASHIN, *J. Appl. Mech., Trans. ASME E84* (1962) 143.
5. Z. HASHIN and S. SHTRICKMAN, *J. Mech. Phys. Solids* **11** (1963) 127.
6. Z. HASHIN, *J. Mech. Phys. Solids* **13** (1965) 119.
7. *Idem, J. Appl. Mech. Trans. ASME E32* (1965) 630.
8. *Idem, AIAA J.* **4** (1966) 1411.
9. S. AHMED and F. R. JONES, *J. Mater. Sci.* **25** (1990) 4933.
10. Z. HASHIN, *Int. J. Solids, Structures* **6** (1970) 539.
11. R. M. CHRISTENSEN, in "Theory of viscoelasticity" 2nd Edn (Academic Press, New York, 1982).
12. *Idem*, in "Mechanics of composite materials" (John Wiley, New York, 1979).
13. G. MILTON, *J. Mech. Phys. Solids* **40** (1992) 1105.
14. R. ROSCOE, *J. Mech. Phys. Solids* **17** (1969) 17.
15. M. AVELLANEDA and G. MILTON, *SIAM J. Appl. Math.* **49** (1989) 824.
16. C. P. CHEN and R. S. LAKES, *Cellular Polym.* **8** (1989) 343.
17. A. S. NOWICK and B. S. BERRY, in "Anelastic relaxation in crystalline solids" (Academic Press, New York, 1972).
18. J. D. FERRY, in "Viscoelastic properties of polymers" 2nd Edn (John Wiley, New York, 1979).
19. R. S. LAKES, J. L. KATZ and S. S. STERNSTEIN, *J. Biomech.* **12** (1979) 657.
20. I. NIELSEN, in "Mechanical properties of polymers" (Reinhold, New York, 1962).
21. A. T. SHIPKOWITZ, C. P. CHEN and R. S. LAKES, *J. Mater. Sci.* **23** (1988) 3660.

Received 26 August
and accepted 17 November 1992